

47 and flows”. Many researchers have conducted empirical studies to explore the “dynamics”
48 of the spatial structure of an urban region, by taking the spatial interaction network
49 approach. A spatial network is typically generated by representing a spatial unit (e.g.,
50 neighborhood, traffic analysis zone, or grid) as the node of a network, and the intensity of
51 flow (people, vehicle, etc.) between nodes as weighted links. The “spatial structure” of an
52 urban area can be detected from such a spatial network (e.g., Liu et al. 2015, Kempinska
53 et al. 2018). The spatial structure of an urban region shapes and is shaped by spatial
54 interaction patterns. Despite potential issues such as data uncertainty (Xu et al. 2020;
55 Steiger et al. 2015; Huang and Wong 2016), spatial network analysis can be used to
56 effectively explore the spatial structure with good performance (Wang et al. 2017, Wang
57 et al. 2019), particularly with increasingly available human mobility data (e.g., taxi GPS
58 trajectories, social media, smart card data, etc.).
59

60 The considerable geographic extent and a “top-down” administrative system are two of the
61 main characteristics of China’s urban agglomeration development (Wu 2002). The Beijing-
62 Tianjin-Hebei urban agglomeration (BTHUG) is the biggest urban agglomeration located
63 in northern China, which includes the national capital, Beijing, the municipality of Tianjin,
64 and the province of Hebei. Many studies in the past tend to explore the spatial structure of
65 the BTHUG through its local social economical factors (Kuang et al., 2014), impervious
66 surface coverage (Cao et al. 2018), and spatial connection intensity (e.g., transport
67 connection and economic connection). However, the main mechanism for urban
68 agglomeration integrated development in China is top-down administrative planning which
69 controlled by central government. Thus, it should be paid attention to how human mobility
70 and spatial interaction can facilitate the spatial structure analysis of BTHUG using the
71 mobile phone dataset under the constraint of top-down administrative planning. The aim
72 of this study is to explore the spatial structure of the BTHUG. The research questions can
73 be summarized as: (1) What are the statistical characteristics of spatial interactions in
74 BTHUG? (2) How these statistical characteristics reflect the spatial structure of BTHUG?
75 (3) Are there significant differences among “top-down” administrative cities and the
76 structures identify by different community detection algorithms (e.g., Infomap, Louvain
77 and Regionalization)? If so, what is the difference? And (4) what is the observed spatial
78 structure of BTHUG shaped by “top-down” administrative planning and the “bottom-up”
79 spatial patterns?
80

81 To answer the questions, this study proposed a spatial network analysis framework based
82 on a large-scale mobile phone dataset. The dataset covers 20 million users (nearly 20% of
83 the BTHUG population) and includes various types of demographic information. It can
84 therefore reflect real-world human mobility patterns. We first extract an origin-destination
85 spatial interaction matrix from the mobile phone dataset to build a spatial interaction
86 network G . A set of network metrics (i.e., degree, strength, a rich-club coefficient, and an
87 assortativity coefficient) are applied to explore statistical characteristics of spatial
88 interaction in BTHUG. The result reveals a *global (core) center* area and the linkages
89 between this and other counties in the BTHUG. Then, the top-down administrative cities
90 and three different outcomes from selected community detection algorithms (i.e., Infomap,
91 Louvain and Regionalization) are compared to further discuss the inconsistency in
92 detecting communities by using different community detection algorithms. Last, the

93 detected communities via Infomap, which has the best match with top-down administrative
94 cities, is applied to identify the *local centers*, *major cities*, and *peripheral cities*. The results
95 provide deeper insights into the urban agglomeration structures and spatial network
96 collaboration.

97 98 **2. Related work on urban agglomeration structures**

99 Traditionally, urban structure refers to the spatial arrangement or layout of land uses, such
100 as zonal (Burgess 2008), sectoral (Hoyt 1939), and multiple nuclei models (Harris and
101 Ullman 1945). Early studies of urban structure mainly focused on static land use at the city
102 level. With the rapid development of information technology and urbanization, big data of
103 the mobility of people, transport vehicles, and freight has become increasingly available.
104 Researchers have begun using big data to detect the dynamics of urban structures through
105 spatial network analysis (e.g., Zhong et al. 2014; Shaw et al. 2016). Hence, the spatial
106 structure of urban regions turns to the arrangement of spatial units (e.g., grid squares,
107 neighborhoods, blocks, etc.) and a set of relationships arising out of the distribution of these
108 units and the underlying interactions. These consist of people, freight, and capital
109 (Rodrigue 2016, Wu 2020). From this perspective, the spatial structure of urban areas both
110 shapes and is shaped by spatial interaction patterns. In terms of the methodology, by
111 extracting the origin-destination (OD) matrices from mobility big data (e.g., taxi GPS
112 trajectories, social media, and smart card data), a spatial interaction network can be
113 constructed that reveals the spatial structure (Louail et al. 2015), in which the ODs are
114 regarded as the nodes of the network.

115
116 The basic properties of spatial networks (i.e., their degree and strength) can provide an
117 overview of travel demand and interactions across urban space (Zhao et al. 2018). Zhong
118 et al. (2014) identified the connectivity and centrality of an urban space using a centrality
119 quantity measurement of the spatial network (i.e., betweenness and PageRank). Wei et al.
120 (2018) found a typical oligarchic spatial structure characteristic in China's population flow
121 network by using the rich-club coefficient and the assortativity coefficient. Unlike the
122 centrality measurement, the rich-club and assortativity coefficients emphasize that a few
123 powerful nodes dominate the structure of a network, and will thus not only form a cohesive
124 cluster among themselves, but will also maintain their connections with peripheral nodes.
125 These coefficients are therefore widely used to explore various types of network structure,
126 such as two-level (e.g., "rich-poor") or hierarchical structures (e.g., Xing et al. 2016,
127 Ducruet et al. 2016).

128
129 The spatial structure in a spatial network can be detected using "community detection"
130 algorithms. This organization can then be projected onto an urban region and depict the
131 borders that subdivide the space into different clusters according to the spatial interaction
132 patterns, which are called the "bottom-up" borders, in contrast to the "top-down"
133 administrative borders (Yin et al. 2017). The hypothesis behind the bottom-up borders is
134 that nodes (i.e., spatial units) with strong interactions will form a module (i.e., community),
135 and the divisions between the modules are the borders. In the past decade, the Infomap,
136 Louvain and Regionalization methods are widely applied to detect the community structure
137 for a spatial network (Guo 2008, Lengyel et al. 2015, Guo et al. 2018).

138

139 Many studies suggest that although the structures of network communities in the
140 geographic space generally correspond well with top-down administrative borders, the
141 presence of inconsistent borders indicates that human movements do not necessarily follow
142 them. First, it has been suggested that closely connected spaces, in the form of network
143 communities, follow the effects of spatial proximity. That is, the interaction strength
144 between two spaces decreases as the geographical distance between them increases
145 (Fotheringham 1981). Second, research demonstrated how the intrinsic demands of human
146 movement and resources (e.g., trade, urban freight) can reshape the structure of space (Ratti
147 et al. 2010, Gao et al. 2013, De Montis et al. 2013).

148
149 Studies using mobility big data analytics and new technological methods have laid the
150 foundations for a better understanding of human mobility behavior, and its relationship
151 with the spatial structure of city regions in particular. However, most have focused on the
152 city level. Some urban agglomerations or city-clusters have emerged, such as the New York
153 bay area, Tokyo bay area, and Yangtze River Delta urban agglomeration. Most countries,
154 including China, break down the urban region space into a system of multi-level
155 hierarchical administrative units (e.g., provinces, prefecture-level cities, counties, and
156 towns). The Chinese government recently initiated a national strategy to establish urban
157 agglomerations, such as the BTHUG, which was first proposed by the central government
158 in 2015 (Zhang 2016). Some researchers have assessed urban agglomeration structures
159 using census or surveying data, but these are costly and time-consuming in the early stage
160 (Castells 2011). Flow data (e.g., taxi GPS trajectories, social media, and smart card data),
161 both within a city and among cities, are becoming increasingly available due to advances
162 in information technology, and thus enable further insights into the structures of cities and
163 city-clusters, and offer unprecedented levels of resolution.

164
165 Current spatial network analysis techniques are convenient for exploring the structure of
166 urban agglomerations because they are often tied to mobility-related big data (e.g., taxi
167 GPS trajectories, social media, smart card data) that can be used to examine spatial
168 interaction patterns (Liu et al. 2012, Liu et al. 2014). However, the use of spatial networks
169 via mobility big data presents a level of uncertainty, as the revealed spatial structure of an
170 urban agglomeration may be affected by the source of the data. For example, social media
171 data (e.g., geo-tagged photos, geo-located tweets) are sparse and irregular in time and space
172 (Xu et al. 2020). In addition, the data sample cannot cover the entire population (i.e., social
173 media data, taxi GPS trajectories, and smart card data only cover specific users). Thus, the
174 identified spatial structure of urban agglomerations based on spatial networks constructed
175 via these datasets may not reflect the spatial interaction patterns in the real world (Steiger
176 et al. 2015, Huang and Wong 2016). This issue has prevented the establishment of a
177 systematic understanding of the spatial structure of urban agglomeration based on spatial
178 interaction patterns. Mobility big data should thus be considered along with various types
179 of demographic information to accurately establish spatial interaction patterns and spatial
180 structures.

181
182 We address these issues by combining mobile phone data with a spatial network approach.
183 We analyze a human mobility dataset that captures the spatial interaction patterns in the
184 BTHUG, and apply methods that can reveal the spatial structure of the BTHUG. We aim

185 to provide an understanding of this structure that is based on real-world spatial interaction
186 patterns.

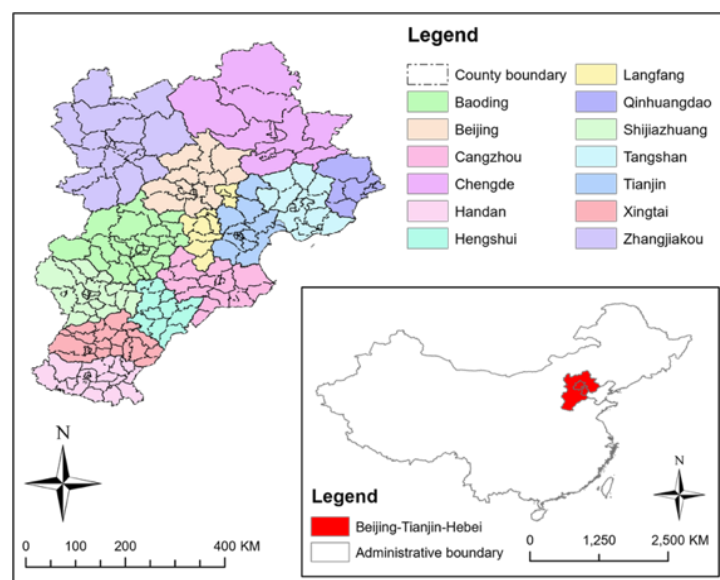
187

188 3. Dataset and spatial network construction

189 3.1 Study area

190 Our study area is the national capital region of China, or the Beijing-Tianjin-Hebei urban
191 agglomeration (BTHUG), which is the biggest urbanized megalopolis in northern China
192 and has an area of 217,156 km² (see figure 1). The BTHUG includes 204 counties that
193 belong to 13 cities. Beijing is the capital and the center of politics, economics, and culture
194 in China. Tianjin is one of the country's four directly governed municipalities (the others
195 are Beijing, Shanghai, and Chongqing), and Hebei is a province with 11 prefecture-level
196 cities. The study area had a population of 110 million and a GDP of CNY66,474 hundred
197 million in 2014.

198



199

200

201

202

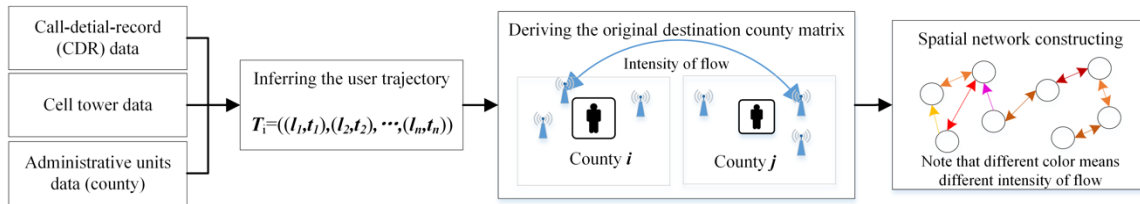
Figure 1. Study area of Beijing-Tianjin-Hebei (BTH) with 13 cities and 204 counties.

203

203 3.2 Dataset and BTHUG spatial network construction

204 Figure 2 presents the details of the dataset and data preprocessing for spatial network
205 construction. The mobile phone data collected by China Unicom Co., Ltd. from November
206 2 to November 7, 2015, constituted the main dataset used in this work. This includes 20
207 million users (nearly 20% of the BTH region's population) and 266,214 cell towers. Note
208 that November 2 to November 7, 2015 are normal weekdays in China. We randomly
209 selected this period after excluding some special holiday periods (e.g., Spring Festival,
210 National Day holidays, etc.). Further, county services as the basic unit in the urban
211 agglomeration integrated development in China (Ma 2005, Yeh and Chen 2020). Hence,
212 the administrative county units of the BTH provide another dataset. Each mobile data
213 record tracks various attributes of a user, such as a unique ID, the date, the time, and the
214 connected cell tower, every 30 minutes or when phone communication starts (i.e., a
215 call/SMS). Note that the users' IDs and cell phone numbers were re-assigned as sequence
216 numbers (e.g., 1, 2, 3...) before data preprocessing to protect personal privacy.

217



218

219

220

221

Figure 2. Details of dataset and preprocessing: (1) Inferring the user trajectory; (2) Deriving the origin-destination county matrix M ; (3) Constructing the weighted-directed spatial network.

222

223

224

225

226

227

228

229

230

231

232

233

234

235

236

To infer each user’s movements among counties, we first perform a spatial join analysis in ArcMap of the association between cell tower data and administrative county units. The cell tower data provide information pertaining to the county that the cell tower is located in. Second, each user’s trajectory among counties is denoted as a tuple list of $T = \{(l_1, t_1), (l_2, t_2), \dots, (l_n, t_n)\}$, where l_i is the user’s location (i.e., county) at time t_i . Third, we infer the stay county chain of each user by setting the stay time threshold to be not less than six hours, and the stay county chain of each user is presented as $L = (c_1, c_2, \dots, c_n)$, where c_i means that the user stayed at county i , and the tuple (c_i, c_{i+1}) is one pair of origin-destination counties in the user’s movement. Note that a user may spend a long time in one county, and so if a user has multiple continuous records in a single county we only consider one entry. Finally, we extract all users’ origin-destination counties from the stay county chain, and the matrix of origin-destination counties is represented as $M = (c_i, c_j, w)$, where c_i is the origin county, c_j is the destination county, and w is the intensity of flow between c_i and c_j .

237

238

239

240

241

242

243

244

To explore the BTHUG structure, we construct a spatial weighted-directed network based on the matrix of origin-destination counties M . First, each county is presented as a node (i.e., c_i is N_i), and the coordinate (x_i, y_i) of its center is regarded as the spatial location of the node. We then assign a directed edge e_{ij} to a pair of nodes (N_i, N_j) depending on whether there was human movement between them or not. The weighted W_{ij} of each edge e_{ij} is given by the intensity of flow w between c_i and c_j . A weighted-directed spatial network $G = (N, E, W)$ is thus obtained.

245

246

247

248

249

250

251

252

Figure 3 demonstrates the spatial interaction patterns using the movement flows on BTHUG. As the figure shows, each node in this graph corresponds to a geographic center of counties. The red lines indicate a higher flow between counties. We observe that slight amounts of counties displayed higher movement flows, including Beijing, Tianjin, Shijiazhuang, which represent the hubs of the whole network. Further, the figure shows that most of the counties in the same cities (e.g., Baoding, Xingtai, Handan, et al.) have higher spatial interaction with each other.

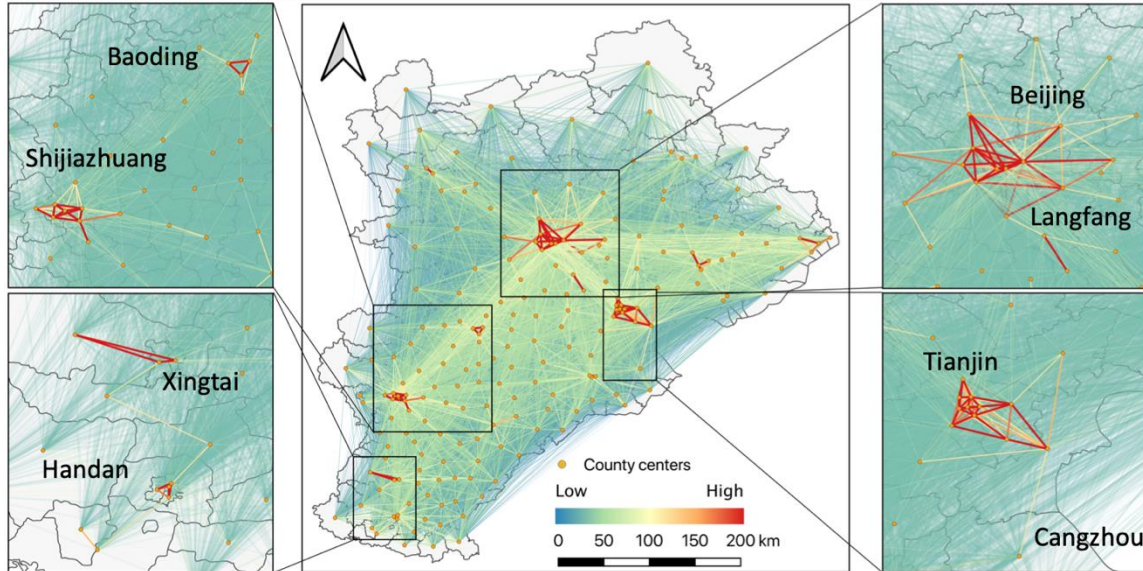


Figure 3. Spatial interaction patterns in BTHUG based on the movement flows.

253
254
255
256
257
258
259
260
261
262
263
264
265
266
267

4 Urban agglomeration structure analysis

In this study, a spatial structure that consists of four city levels are defined to better understand the agglomeration structure:

- Global (core) center: an area that comprises a number of cities (nodes) that have the *largest* volume of human flow and *strong* linkages among them.
- Local center: an area that comprises a number of cities (nodes) that has *large* human flow and *strong* linkages with the global center.
- Major cities: cities that have *low* human flow and *strong* linkages with global and local centers.
- Peripheral cities: cities that have *low* human flow and *weak* linkages with global and local centers.

268 Given the spatial network G constructed in section 3, where the administrative geographic
269 units (i.e., county in G) are presented as a node, and intensity of human movements is
270 directed-weighted link between a pair of nodes. A spatial network analysis framework is
271 developed to explore the urban agglomeration structure (see figure 4). There are three steps
272 in this framework: 1) exploring the spatial structure based on spatial network metrics,
273 which includes degree, strength, rich-club coefficient and assortativity coefficient; 2)
274 applying three different community detection algorithms to delineate the organization of
275 urban agglomeration structure; 3) comparing the detected communities from the selected
276 community detection algorithms. The detail of each step is illustrated as follows.

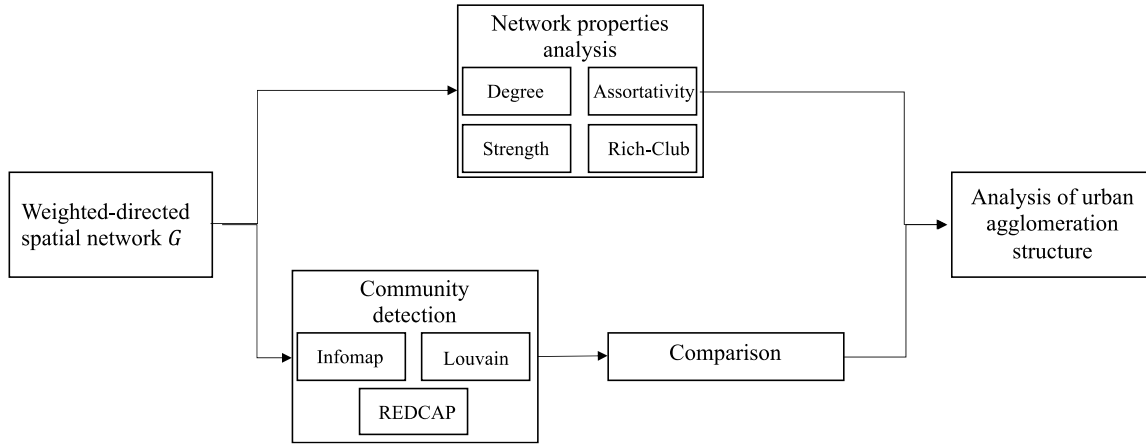


Figure 4. Workflow of empirical analysis.

4.1 Characterizing structure of spatial network

We characterize the BTHUG structure using the metrics of spatial network G . The degree, strength, rich-club coefficient, and assortativity coefficient are applied to reveal the *global (core) center* area and the linkages between this and other counties in the BTHUG.

(1) The *degree* d of a node refers to the number of edges connected to it. The degree distribution $P(d)$ is the proportion of nodes with degree d in the network. We further divide degree into out-degree and in-degree, according to the direction of human movement between each pair of nodes.

(2) The *strength* s of a node refers to the sum of the weights of all edges connected to it. The strength distribution $P(s)$ is the proportion of nodes with strength s . Again, the strength of each node is subdivided into out-strength and in-strength.

(3) The *rich-club coefficient* is an effective tool to measure the structural characteristics of a network based on *degree* d or *strength* s . This can reveal “rich-member” nodes, which are subgroups of powerful nodes that preferentially and intensely connect with each other, while they maintain connections with “poor” nodes (Colizza et al. 2007, Van Den Heuvel and Sporns 2011, Alstott et al. 2014). Nodes with a strength greater than a certain value of r are typically considered as rich nodes, and thus r can be used to define rich nodes (e.g., those with high d or s). The rich-club coefficient is measured using the global and the local rich-club coefficient value, ϕ_{local} (Opsahl et al. 2008, Opsahl 2009).

(4) The *assortativity* represents how nodes tend to connect with other nodes that have similar degrees, whereas *disassortativity* is the characteristic of nodes tending to connect with others that have different degrees. It is widely used to measure the network structural characteristics and is defined as the Pearson correlation coefficient of degree between pairs of linked nodes (Newman 2002, Xu et al. 2010). The assortativity value is expressed as a scalar value, ρ , in the range from -1 to 1. A positive value of ρ means a network is characterized by assortativity, with a negative value indicating disassortativity. For a directed network, the assortativity can be measured with degree, in-degree and out-degree. Thus, a global assortativity and four directed assortativity (i.e., $\rho(\text{out}, \text{in})$, $\rho(\text{in}, \text{out})$, $\rho(\text{out},$

312 out), and $\rho(\text{in}, \text{in})$ can be estimated to quantify the tendency of nodes with un-directed and
313 directed methods in a network (Foster et al., 2010).

314

315 **4.2 Community detection methods**

316 As discussed in Section 2, the bottom-up border of a community's structure in a spatial
317 network can be identified using community detection algorithms. In this work, the Infomap,
318 Louvain and Regionalization methods are applied to the spatial network G to detect how
319 communities are organized (i.e., *local centers*, *major cities*, and *peripheral cities*). The
320 detail of each method is introduced as follows.

321 **4.2.1 Infomap community detection algorithm**

322 The Infomap algorithm proposed by Rosvall and Bergstrom (2008) is focused on revealing
323 community structure in weighted and directed networks. The main idea is that the
324 interaction flow can be measured based on the probability flow of random walks in a
325 network, and the network can be decomposed into modules by making the interaction flow
326 inside a community significantly larger than those between communities. Nodes in the
327 network are first given a unique code according to the visiting frequency of the random
328 walk. Huffman coding is then used to assign more frequently visited nodes a shorter code,
329 and thus the random walk trajectory of a network can be described as the prefixed
330 community code plus the suffixed code of nodes inside the communities. Finally, the
331 communities are clustered by finding the minimum description code length. The average
332 trajectory length of the code describing a step of the random walk is estimated using the
333 following map equation:

334

$$335 \quad L(M) = qH(Q) + \sum_{i=1}^m p_i H(p_i) \quad (1)$$

336

337 where $L(M)$ is the expectation of the average trajectory length of code spent on a random
338 walk inside and outside communities, $qH(Q)$ is the entropy of movement among clusters,
339 and $\sum_{i=1}^m p_i H(p_i)$ is the entropy of movement within clusters. Specifically, q is the
340 probability that a random walker moves from one cluster to another, whereas p_i is the
341 probability of movement within cluster i .

342

343 **4.2.2 Louvain community detection algorithm**

344 The Louvain algorithm proposed by Blondel et al. (2008) and extended by Leicht and
345 Newman (2008) is a classic of modularity optimization methods on community detection
346 algorithms for an undirected network. The algorithm was then adjusted by Dugué and Perez
347 (2015) to compute communities for a directed network. Specially, the modularity
348 optimization method provides a way to assess the existence of an edge between two nodes
349 in a directed network by comparing it with the probability of have such an edge in a random
350 model following the same degree distribution than the original network. For instance, if
351 two nodes i and j have small in-degree/large out-degree and small out-degree/large in-
352 degree, then having an edge from i to j should be considered more surprising than having
353 an edge from j to i . In this study, the modularity Q of a partition C for the spatial network
354 G is defined as follows:

355

$$Q = \frac{1}{W} \sum_{ij} (w_{ij} - \frac{s_i^{in} s_j^{out}}{W}) \delta(c_i, c_j) \quad (2)$$

where W stands for the sum of weighted for edges in G . w_{ij} is the weight associated to the edge connecting the node i and the node j . s_i^{in} and s_j^{out} are the in-strength and out strength of node i and j , respectively. The function $\delta(c_i, c_j)$ is defined as 1, when nodes i and j belong to same community, and 0 otherwise.

4.2.3 Regionalization

Regionalization with dynamically constrained agglomerative clustering and partitioning (REDCAP) is a family of regionalization methods based on spatially constrained hierarchical clustering (e.g., single linkage (SKL), complete-linkage (CLK), and average-linkage (ALK) methods) (Guo 2011). To apply the regionalization method to the spatial network G , a similarity measure is defined for each pair of nodes (i.e., counties). This work applies the concept of modularity measures, which is defined as follows:

$$Modularity_{ij} = Obserflow_{ij} - Estflow_{ij} \quad (3)$$

$$Estflow_{ij} = \frac{p_i p_j}{d_{ij}^\beta} \quad (4)$$

where $Obserflow_{ij}$ is the observed flow between node i and j , and $Estflow_{ij}$ represents the expected flow between node i and j under the gravity model (i.e., equation (4)); p_i and p_j are the population in county i and j ; d_{ij} is the spatial distance between node i and j , and the β is distance-decay parameter obtained by fitting a gravity model (Kang et al. 2013).

After estimating the modularity measure for each pair of counties in BTHUG, we have a weighted matrix for each link of counties, where the higher the modularity, the stronger the connection between the two counties is. Given the modularity matrix, an average-linkage clustering based regionalization method (i.e., full-order-ALK) is used to detect the community for the spatial network G . There are two steps in the method: (1) the first step builds a hierarchy of clusters from the bottom up via iteratively merging the most connected clusters based on the county to county modularity values, and the output is a spatially contiguous tree; (2) the second step partitions the spatially contiguous tree to obtain community while maximizing within-community modularity and enforcing the spatial contiguous constraints (i.e., the detected communities should consist of spatially contiguous counties).

4.3 Comparing the selected community detection methods

As this section 2 mentioned, many studies suggest that the structures of network communities in the geographic space generally correspond well with top-down administrative borders. One of the reasons is that the spatial structure is both shaped by "top-down" administrative planning and the "bottom-up" spatial patterns. Especially, it suggests that close spaces will be connected, in the form of network communities, follow the effects of spatial proximity. Because the interaction strength between two spaces

400 decreases as the geographical distance between them increases. Hence, to quantitatively
401 compare the quality of the communities detected by the selected community detection
402 methods, we estimate the similarity of spatial distribution to evaluate how well the detected
403 communities match the top-down administrative cities. We first use $link_{ij}$ to present
404 whether counties i and j belong to the same community/city (i.e., $link_{ij} = 1$, when counties
405 i and j belong to the same community/city, and 0 otherwise). Then, the outcomes from the
406 selected community detection methods can be represented as various matrices M_{Info} ,
407 $M_{Louvain}$, and M_{REDCAP} . Note that the top-down administrative cities composed of counties
408 are also represented as a matrix M_{city} . Last, bivariate Pearson correlation analysis is
409 applied to investigate the similarity of spatial distribution between each matrix with each
410 other. The higher the Pearson correlation coefficient is, the better the detected communities
411 match with each other. It should be noted that the three selected community detection
412 methods are sensitive to resolution parameters or multiple implementations, which
413 indicates that the detected communities cannot always converge the same result under
414 different parameters or after multiple implementations. Hence, only results that have the
415 best match with top-down administrative cities after hundred implementations with
416 different parameters will be selected to further compare with others.

417

418 **5. Results and discussion**

419 In this section, we explore the BTHUG structure characteristics based on the constructed
420 spatial network of human mobility $G = (N, E, W)$, which was introduced in subsection 3.2.

421

422 **5.1 Spatial network construction and characterization**

423 As introduced in subsection 4.1, we select degree, strength, the rich-club coefficient, and
424 the assortativity coefficient to detect the *global (core) center* and the linkages between the
425 global center area and other counties in the BTHUG. The statistical characteristics of
426 degree and strength are first calculated to explore the human movement patterns. As Figure
427 5(a) shows, the cumulative probability curves of degree range from 225 to 406 and decay
428 slowly. We also find that the nodes with a higher degree ($d \geq 370$) count for a large
429 proportion, which is 73%. The results indicate that the majority of counties among the
430 BTHUG have linkages with other counties. However, Figure 5(b) shows that the nodes
431 with a higher strength ($s \geq 100000$) account for a tiny percentage, which is 6.9%. Thus,
432 a minority of counties in the BTHUG have larger and more frequent flows with other
433 counties. A few developed counties therefore dominate the BTHUG structure with a very
434 large number of human movements.

435

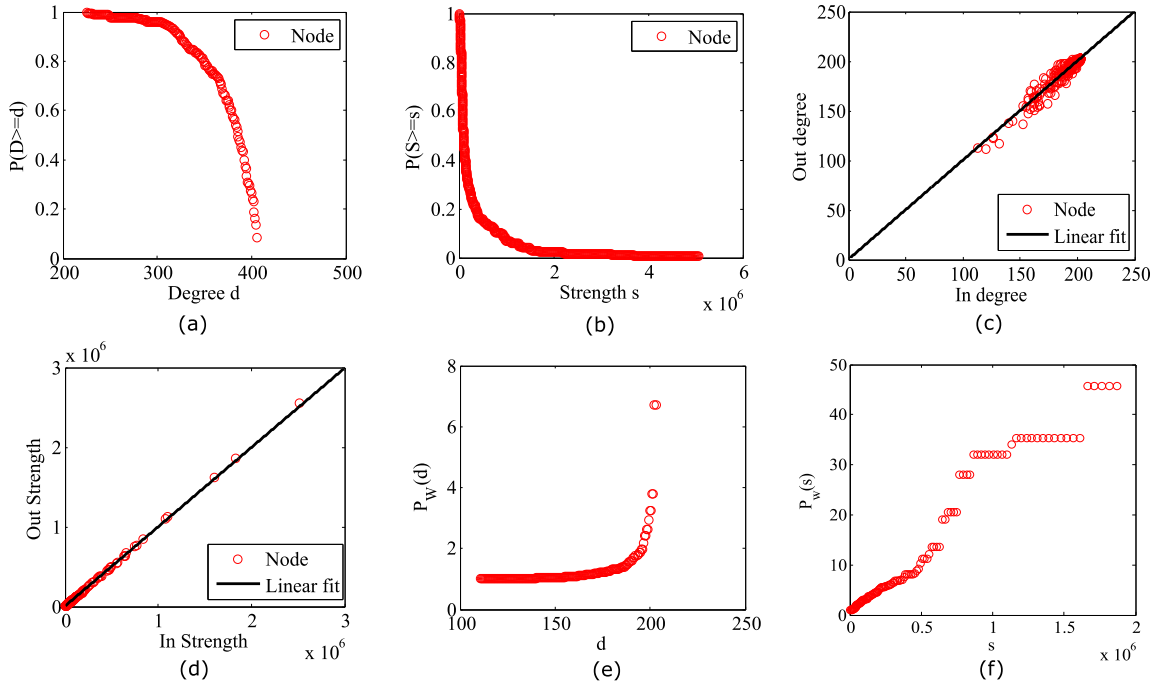


Figure 5. (a)-(b) Cumulative probability distributions of degree and strength; (c)-(d) Correlations between in/out degree and strength; (e)-(f) Rich-club coefficients when $r = d$ and $r = s$.

436
437
438
439

440 The constructed spatial network G is directed, so degree and strength can be further divided
441 into in/out degree and strength, and we further explore their correlations. As shown in
442 Figures 5(c) and 5(d), in-degree is strongly linearly correlated with out-degree, and the
443 same true for in-strength and out-strength. All of the points are distributed on both sides of
444 the line $y \sim x$, and the goodness of fit attained is above 0.92. These findings indicate that
445 human movement is mutual among counties in the BTHUG. For two given counties, the
446 human movement flows between them in both directions have no significant difference in
447 terms of quantity in most cases.

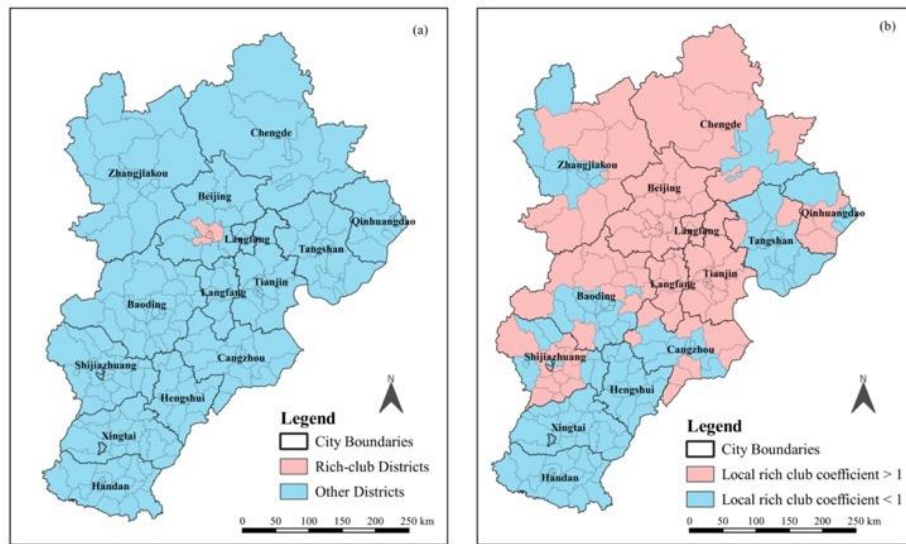
448

449 The above results reveal that a few developed counties dominate the BTHUG structure
450 with a very large number of human movements. The rich-club coefficient and assortativity
451 coefficient are examined to further detect the dominant counties (i.e., the global center).
452 Figures 5(e) and (f) present the global rich-club coefficients, and both $P_w(d)$ and $P_w(s)$
453 are greater than 1 and reveal a general upward trend, confirming the existence of an obvious
454 rich-club effect in BTHUG. The results also reveal a significant “elbow point” feature in
455 the changes for both the $P_w(d)$ and $P_w(s)$ curves.

456

457 In Figure 5(e), $d = 200$ is an important elbow point. When degree d is larger than 200 the
458 curve rapidly rises. In Figure 5(f), the curve has a hierarchical upward trend. When $s <$
459 6.3×10^5 , the curve continues to rise smoothly. The curve then jumps when $s > 6.3 \times$
460 10^5 and reaches its peak when $s > 1.6 \times 10^6$. According to the results, we identify
461 Chaoyang, Xicheng, Dongcheng, Fengtai, and Haidian (Figure 6 (a)) as the “rich-club”
462 counties (i.e., the global center area) that have the most connected and powerful spatial
463 interactions in the BTHUG. The rich-club counties are defined as those with $d > 200$ and

464 $s > 1.6 \times 10^6$. Note that all of these counties are in Beijing, and Chaoyang is the heart of
 465 the BTHUG with the maximum strength, $s = 5 \times 10^6$.
 466



467
 468
 469 Figure 6. Rich-club coefficients of cities in BTH region: (a) Rich-club members in global rich-club
 470 coefficients; (b) Local rich-club coefficients.
 471

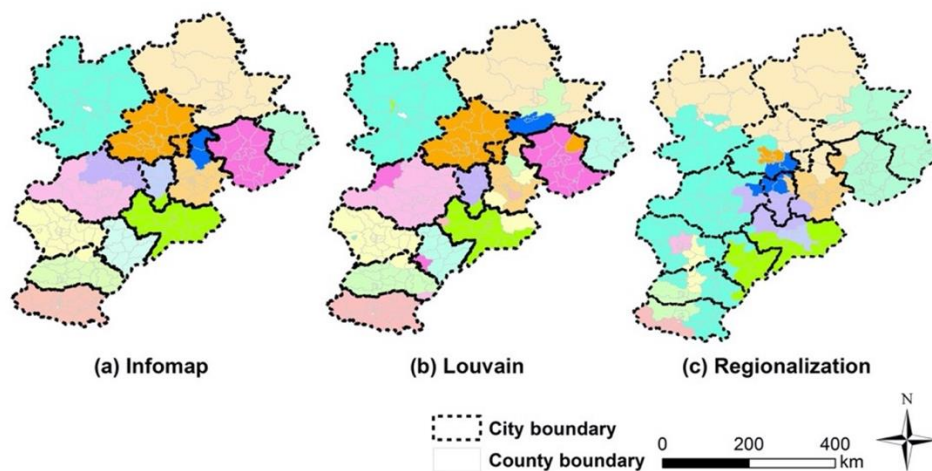
472 The global assortativity coefficient is -0.183, and the directed assortativity coefficients are
 473 -0.183, -0.176, -0.179 and -0.179 for $\rho(out,in)$, $\rho(in,out)$, $\rho(out,out)$, and $\rho(out,out)$,
 474 respectively. The results are consistent with the strongly linear correction among in-out
 475 degree and in-out strength, which suggests that human movement is mutual among counties
 476 in the BTHUG. Further, the assortativity coefficients indicate that the BTHUG structure
 477 has relatively weak disassortativity. The non-rich nodes with low degrees tend to be
 478 connected to the rich nodes, and vice-versa (Colizza et al. 2006). This is consistent with
 479 the rich-club analysis; the rich nodes connect strongly with one another, and thus the human
 480 movement flows are highly central among rich-club counties in the BTHUG. The local
 481 rich-club coefficient of each node is inferred based on the method given in section 4.1.
 482 Figure 6(b) shows the result divided into two groups according to the values of the local
 483 rich-club coefficients: $\phi_{local} > 1$ and $\phi_{local} < 1$. The counties in the $\phi_{local} > 1$
 484 group tends to connect with rich nodes, whereas the others tend to connect with non-rich nodes.
 485 The spatial distribution between the two groups obviously differs. Counties in the $\phi_{local} >$
 486 1 group are mainly concentrated around Beijing. Specifically, it expands from the five rich-
 487 club counties (Chaoyang, Xicheng, Dongcheng, Fengtai, and Haidian), and includes four
 488 exclaves (i.e., eastern Chengde, northern Qinhuangdao and Cangzhou, and Shijiazhuang).
 489 A $\phi_{local} < 1$ group is situated in the southern part of the BTHUG. This indicates that direct
 490 interactions between southern counties and rich BTHUG members are weaker. Distance
 491 decay may account for this. People in the southern part of the BTHUG tend to go to their
 492 neighboring $\phi_{local} > 1$ region (e.g., Shijiazhuang), which has strong direct linkages with
 493 rich members, and thus form a hierarchical structure.
 494

495 **5.2 Results of community detection**

496 Before performing the selected community detection methods, we first estimate the
497 expected flow using the gravity model, and then calculate the modularity following the
498 method given in section 4.2.3. We find that the expected flow estimated using the gravity
499 model has a strong linear correlation (i.e., $R^2=0.84$ and $p\text{-value} < 0.01$) with the observed
500 flow (shown in Figure S1). This confirms that the intensity of human spatial interactions
501 between two counties decreases as the geographic distance between them increases in
502 BTHUG. Then, we find that the expected flow may underestimate among counties with
503 large geographic distance (i.e., modularity > 0 , shown in Figure S2) and overestimate
504 among counties with smaller geographic distance (i.e., modularity < 0 , shown in Figure S3).

505
506 As section 4.2 introduced, we detected the community structure of the spatial network G
507 with the three selected methods: Infomap, Louvain, and Regionalization (i.e., full-order-
508 ALK). It should be noted that only results that have the best match with top-down
509 administrative cities after hundred implementations with different parameters will be
510 selected to further compare with others. Figure 7 shows the results of the community
511 detection for the spatial network G . Each discovered community is represented by a unique
512 and randomly assigned color. The results show that the detected communities from
513 Infomap and Louvain generally correspond well with the administrative city boundary. The
514 major different parts between infomap and Louvain is Tianjin city, it has been divided into
515 northern and southern parts of Tianjin by infomap, while the Louvain divides Tianjin into
516 four non-spatially adjacent communities. Meanwhile, the spatially adjacent counties are
517 grouped into the same community by using infomap and Regionalization. It is reasonable
518 that the results of infomap group the spatially adjacent counties into the same community
519 since the intensity of human spatial interactions between two counties decreases as the
520 geographic distance between them increases in BTHUG (as the above gravity model
521 revealed). Further, using Regionalization method will generate a more geographically
522 compact region. The results show that the detected community detection by different
523 community detection methods for the same spatial network are mostly different. Therefore,
524 it is worth comparing these methods with top-down administrative cities for investigating
525 the urban agglomeration structure.

526



527
528
529

Figure 7. The results of different community detection and regionalization methods: (a) Infomap algorithm; (b) Louvain detection algorithm; (c) Regionalization method (i.e., full-order ALK).

530 To quantitatively compare the quality of the communities detected by the selected
 531 community detection methods, we use the similarity of spatial distribution to evaluate how
 532 well the detected communities match the top-down administrative cities. Specifically, we
 533 perform bivariate Pearson correlation analysis between each pair of them. Table 1
 534 illustrates the results, which indicates that all of the pairs have significant correlations (i.e.,
 535 p -value < 0.05). Especially, the Infomap and Louvain have higher (i.e., 0.87 and 0.79)
 536 Pearson correlation coefficient with top-down administrative cities, while the
 537 Regionalization method has the lowest one (i.e., 0.34). In addition, we apply adjusted Rand
 538 Index (RI) analysis to verify the results of bivariate Pearson correlation. RI analysis is a
 539 method to assess the similarity between two clusters (Rand 1971, Steinley 2004). It ranges
 540 from 0 to 1, and 1 stands for perfect match. Table S1 presents the results of RI analysis,
 541 which is consistent with results of bivariate Pearson correlation analysis.

542
 543 The results indicate that using Regionalization method will generate more geographically
 544 compact regions which are quite different from top-down administrative cities in BTHUG.
 545 Moreover, since the spatial structure is both shaped by "top-down" administrative planning
 546 and the "bottom-up" spatial patterns. Thus, we select the detected communities from
 547 Infomap which has the highest association with top-down administrative cities to further
 548 analyze the urban agglomeration structure in the next section.

549
 550 Table 1. The results of the bivariate Pearson correlation analysis between each pair of the methods

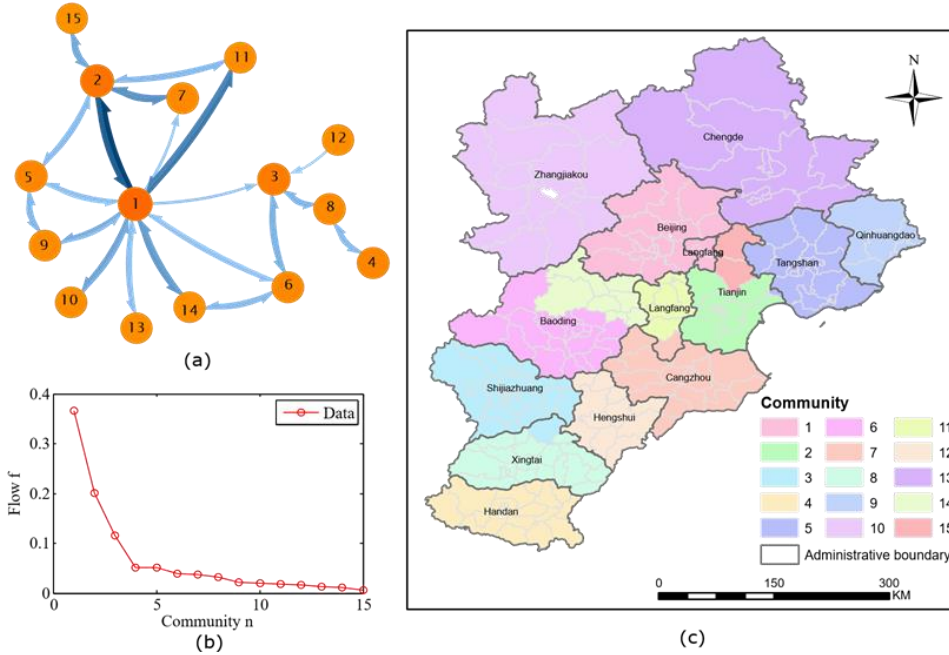
	<i>City</i>	<i>Infomap</i>	<i>Louvain</i>	<i>REDCAP</i>
<i>City</i>	-	0.87*	0.79*	0.34*
<i>Infomap</i>	-	-	0.83*	0.35*
<i>Louvain</i>	-	-	-	0.31*
<i>REDCAP</i>	-	-	-	-

* p -value < 0.05 .

551
 552
 553
 554
 555
 556
 557
 558
 559
 560
 561
 562
 563
 564
 565
 566
 567
 568

5.3 Spatial structure identification

The above results reveal that the spatial interaction reforms the BTHUG into a hierarchical structure. Further, the comparison result of three selected community detection methods suggests that the detected communities from Infomap method are selected to further analyze the urban agglomeration structure. Figure 8 shows the distribution characteristics of 15 communities identified by the method in geographical and network space, and the share of the total flow of each community in the BTHUG (i.e., the sum of flow related to a community divided by the total flow in the BTHUG). Note that the sequence of communities' numbers follows the share of the flow of each community in the BTHUG (i.e., community 1 has the largest share of the flow). Figures 8(a) and (c) show that there is a hierarchical network structure. Figure 8(b) shows the distribution of the share of the flow of each community in the BTHUG. Beijing and northern Langfang (i.e., community 1) consist of the rich-club counties (i.e., the global center area) with the most connected and powerful spatial interactions, so we regard community 1 to be the *global center* of the BTHUG.



569
570
571
572
573
574
575
576
577
578
579
580
581
582
583
584
585

Figure 8. Community detection: (a) communities in network space; (b) percentage of total flow distribution in communities; (c) spatial distribution of communities.

Community 2 (southern Tianjin) and community 3 (Shijiazhuang) in Figure 8(c) are selected as *local centers* according to their share of the flow and their linkages with the global center in the BTHUG. The *major cities* include communities 5 (Tangshan), 6 and 14 (Baoding), 7 (Cangzhou), 9 (Qinhuangdao), 10 (Zhangjiakou), 11 (southern Langfang), 13 (Chengde), and 15 (northern Tianjin). Note that the major cities are defined as in the $\phi_{local} > 1$ group in section 4.1, and have strong and direct linkages with rich-club members (i.e., the global center). The *peripheral cities* contain communities 4 (Handan), 8 (Xingtai), and 12 (Hengshui). Note that the peripheral cities are located in the southern part of the BTHUG and have weaker linkages with the global center. Table 2 gives the details of the hierarchical BTHUG structure.

Table 2. Description of the 4-level hierarchical spatial structure of the BTHUG

<i>City</i>	<i>Community</i>	<i>Level</i>	<i>Share of the flow of each community in the BTH region</i>
<i>Beijing and northern Langfang</i>	<i>1</i>	Global center	38%
<i>Southern Tianjin</i>	<i>2</i>	Local center	20%
<i>Northern Tianjin</i>	<i>15</i>	Major city	1%
<i>Shijiazhuang</i>	<i>3</i>	Local center	13%
<i>Handan</i>	<i>4</i>	Peripheral cities	4%
<i>Tangshan</i>	<i>5</i>	Major city	4%
<i>Baoding</i>	<i>6</i>	Major city	3%
	<i>14</i>	Major city	1%
<i>Cangzhou</i>	<i>7</i>	Major city	3%

<i>Xingtai</i>	8	Peripheral cities	3%
<i>Qinhuangdao</i>	9	Major city	3%
<i>Zhangjiakou</i>	10	Major city	3%
<i>Southern Langfang</i>	11	Major city	2%
<i>Hengshui</i>	12	Peripheral cities	1%
<i>Chengde</i>	13	Major city	1%

586

587 Figure 8(b) indicates that the counties in three centers (i.e., the global center and two local
588 centers) account for 71% of the human movement flows. The remaining counties account
589 for 29% of the human movement flow in the BTHUG, and most movement in these
590 counties is related to the three centers. Community 4 (i.e., the southernmost peripheral city,
591 Handan) has a larger human movement flow but is defined as one of the *peripheral cities*
592 in the hierarchical structure.

593

594 Figure 8(c) reveals that most of the 15 communities correspond well with the
595 administrative city units, except that Tianjin and Baoding are divided into 2 distinct
596 communities, and 3 counties of Langfang are merged with Beijing and Cangzhou. People
597 from a county tend to go to neighboring counties, and particularly among those that have
598 strong linkages in the same administrative city, as they share the same local “Hukou”
599 system.

600

601 However, there are also strong incentives to cross the top-down administrative city units,
602 and the center areas (i.e., the global center and two local centers) are attractive as they
603 provide more employment opportunities and resources. The results suggest that human
604 movement is generally constrained by the top-down administrative city units, but that there
605 are strong incentives to break through this constraint and reshape the spatial structure.

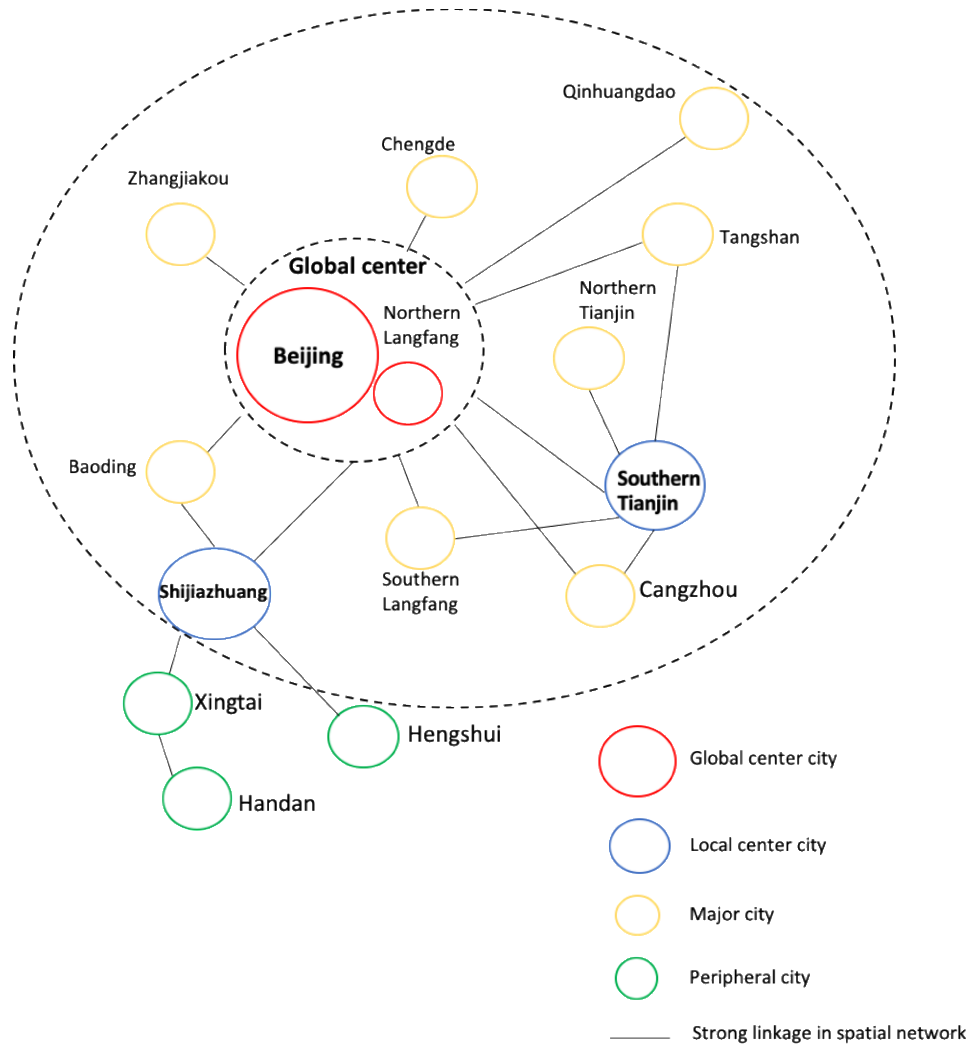
606

607 Figure 9 illustrates the structure of the BTHUG from the perspective of network analysis.
608 The colors and sizes of the icons indicate the roles of cities in the BTHUG structure. Note
609 that the cities’ positions are arranged according to their relative geographical location, and
610 only strong linkages between cities/nodes are visualized, whereas the weak linkages are
611 not shown.

612

613 Figure 9 clearly shows the BTHUG structure and the relative geographical location of the
614 urban agglomeration defined in this study. The *global center* consists of the whole of
615 Beijing and northern Langfang, as Beijing is the national capital and is therefore the
616 economic, cultural, and educational center of the country. Northern Langfang is adjacent
617 to Beijing, and the government promotes the integrated development of Beijing and
618 northern Langfang in its top-down administrative urban planning approach. Tianjin is
619 divided into northern and southern parts, and the latter is one of the two *local centers*.
620 Southern Tianjin has dense and well-built commercial and trade-port areas, which have
621 benefited from the policy resources provided by the central government (e.g., Binhai New
622 Area). Although the top-down policy has encouraged the development of northern Tianjin,
623 it has not formed an integrated development trend with southern Tianjin from the
624 perspective of spatial interactions. Another *local center* is Shijiazhuang, the capital city of

625 Hebei province. Unlike the global center (i.e., Beijing and northern Langfang) and southern
 626 Tianjin, Shijiazhuang is located in the southwestern part of the BTHUG. It is an economic,
 627 cultural, and educational center in Hebei province, and has strong linkages with the global
 628 center and the southern cities of Hebei (i.e., Baoding, Xingtai, and Hengshui).
 629



630
 631
 632
 633

Figure 9. The hierarchical structure in the BTHUG.

634 Northern Hebei province contains the eight major cities of Tangshan, Baoding, Cangzhou,
 635 Qinhuangdao, Zhangjiakou, southern Langfang, Chengde, and northern Tianjin. These
 636 have strong connections with the global and local centers. The global center, local centers,
 637 and major cities form a hierarchical structure of integrated development in the BTHUG
 638 from the perspective of spatial interaction. The peripheral cities are those in the southern
 639 part of Hebei province (i.e., Handan, Xingtai, and Hengshui), and their linkages with the
 640 global center are weaker. The mobile phone big data-driven spatial interaction network
 641 plays a key role in the identification of the hierarchical structure of the BTHUG. Our results
 642 therefore provide new insights into the top-down urban agglomeration plans for the
 643 integrated development of the BTHUG.

644 **6. Conclusion**

645 In this study, we explore the spatial structure of the BTHUG using a proposed spatial
646 network analysis framework based on a large-scale mobile phone dataset, which covers 20
647 million mobile phone users in the BTHUG. The spatial network framework can be applied
648 to other spatial scales (e.g., intra-urban, inter-urban, nationwide) for spatial structure
649 analysis, and other spatial interaction analyses of areas such as trade, public transportation,
650 or urban freight logistics. During the past 40 years since the opening-up of China, the
651 dramatic increases in flows of people, vehicles, goods, and capital have reshaped China's
652 urban agglomeration structure along with the top-down administrative urban
653 agglomeration planning approach of the central government. Thus, discussions about the
654 urban agglomeration spatial structure for the BTHUG are rooted in the particular context
655 of spatial interaction patterns in a spatial network.

656
657 We first construct a spatial weighted-directed network G , derived from over 20 million
658 mobile phone users as they move among the counties in the BTHUG. By computing the
659 spatial network degree, strength, rich-club coefficient, and assortativity coefficient, we
660 observe a hierarchical urban structure shaped by human movement, and a "rich-member
661 club" (i.e., the global center area) consisting of a few counties in Beijing, which are central
662 to the BTHUG. In addition, three selected community detection algorithms are applied and
663 compared to detect the organization of community structure in BTHUG. The results
664 indicate using different community detection methods for a spatial network yield
665 significantly different communities structure. Especially, using Infomap and Louvain
666 algorithms will detect spatially similar community detection, which also corresponds well
667 with top-down administrative cities. Meanwhile, using Regionalization method will
668 generate more geographically compact regions which are quite different from top-down
669 administrative cities in BTHUG.

670
671 Then, the detected community from Infomap which has the highest association with top-
672 down administrative cities has been selected to further analyze the urban agglomeration
673 structure. The Infomap algorithm identifies a hierarchical spatial structure consisting of 15
674 communities for the spatial network G , which are consistent with the top-down
675 administrative city structure. The hierarchical spatial structure consists of one global center,
676 two local centers, major cities with strong linkages with the centers, and peripheral cities
677 that have weaker linkages with the centers. It should be noted the observed spatial structure
678 of BTHUG is consistent with Zhu et al. (2020) by using social economical and transport
679 dataset. The results also suggest that the top-down administrative city unit restricts human
680 movement in terms of spatial interaction, but such movement tends to break through this
681 constraint and reshape the spatial structure.

682
683 These empirical findings can remind policy-makers that it is necessary to rethink whether
684 the administrative planning during the wave of urban agglomeration development is in fact
685 rooted in spatial interaction patterns, or is only "a forced marriage" from the top-down.
686 Especially, the results obtained in this study implies that the spatial structure of BTHUG is
687 over-dependent on the Global center (i.e., Beijing and northern Langfang), which may lead
688 to more series issues in Beijing urban sustainable development (e.g., traffic congestion and
689 air pollution) (Xu et al. 2019, Zhao and Hu 2019). Further, although the top-down policy

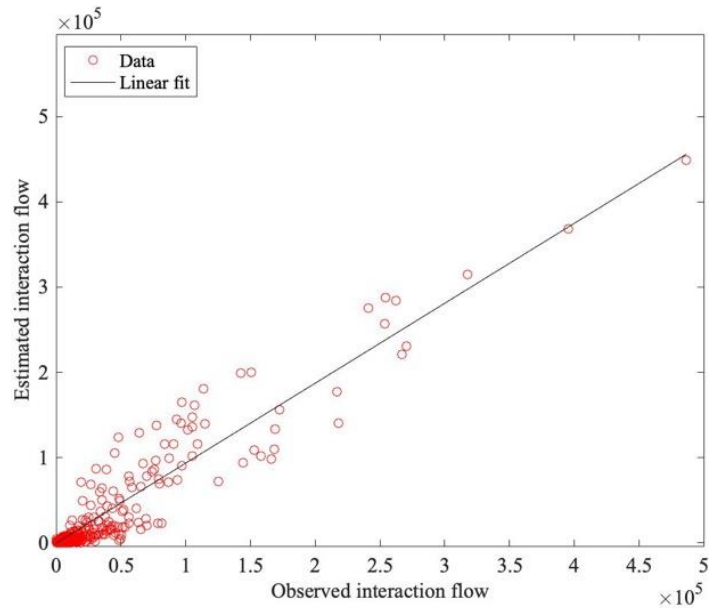
690 has encouraged the development of northern Tianjin, it has not formed an integrated
691 development trend with southern Tianjin from the perspective of spatial interactions. It
692 suggests that ignoring spatial interaction patterns in BTHUG development may lead to
693 ineffective integrated development. Our research also identifies the necessity to consider
694 spatial interaction patterns together with this top-down planning approach in future
695 research into urban agglomeration integrated development.

696
697 Our study has the following limitations. First, there is much potential to further extend our
698 case study on the evolution of the BTHUG structure. Unfortunately, we are limited by the
699 availability of data. By collecting multi-year data, our spatial network method could be
700 extended to investigate how human movements break down the constraints of city borders
701 and reshape the structure of the BTHUG year by year. Meanwhile, our data source has been
702 widely recognized as producing valuable material for large-scale (e.g., inter-county
703 interaction) geographical research, as it covers the population with comprehensive
704 demographic information, but mobile phone data only provide information about user
705 movement without details of transportation behavior (e.g., driving, rail, or public transit).
706 This data characteristic limits the correlation between the BTHUG structure and
707 transportation networks. Further, in spatial terms, a comparative analysis of urban
708 agglomeration structures could be conducted based on our method, if other data (e.g., from
709 the Yangtze River Delta or the Guangdong-Hong Kong-Macao Greater Bay Area) can be
710 collected.

711
712 Finally, since the Infomap and Louvain cannot always converge the same result, it is
713 necessary to implement multiple times to generate a stable result (as we demonstrated in
714 section 4.3). However, the Infomap and Louvain used in this study still can allow
715 researchers to explore the spatial structure. Because the results obtained by Infomap and
716 Louvain in this study are consistent with those obtained using other mobility data source
717 (e.g., social media and smart card data), which report that the detected communities in the
718 geographic space generally correspond well with top-down administrative borders (Zhong
719 et al. 2014, Lengyel et al. 2015, Yin et al. 2017). Future studies would, of course, benefit
720 from developing more stable and insensitive community detection algorithms.

721
722 **Funding:** This research was supported by a grant from RGC Early Career Scheme (Grant
723 no. P0030875).

724
725 Appendix A



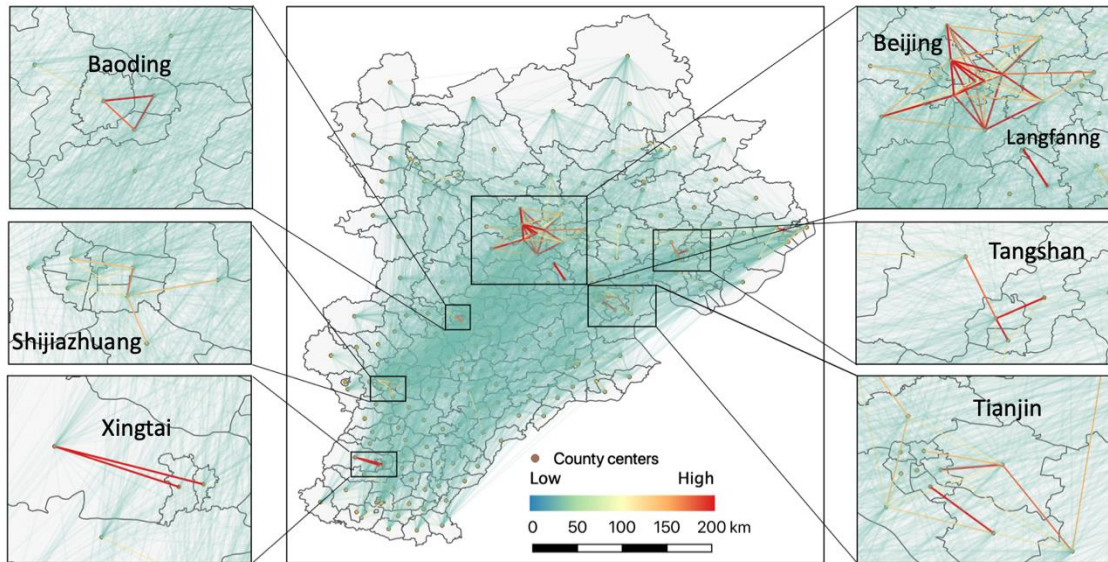
726

727

728

729

Figure S1. The observed interaction strength versus the estimated ones from the adopted gravity model with a fitted $\beta = 0.9$. The dark line indicates strong linear correlation between the estimated and observed interaction strength with $R^2=0.84$ and $p\text{-value} < 0.01$.

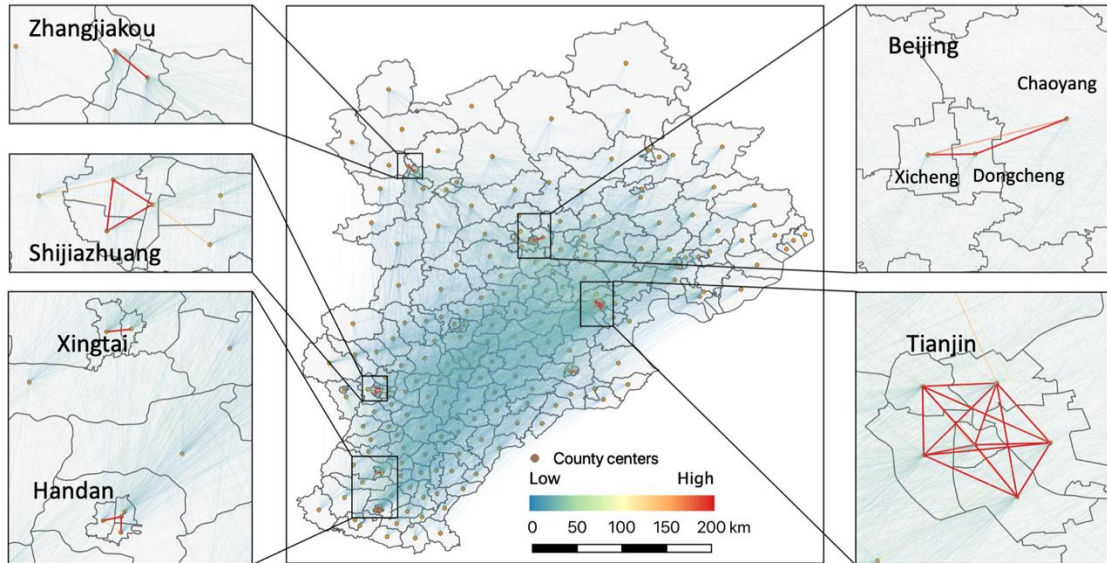


730

731

732

Figure S2. The observed interaction strength which is larger than the estimated ones from the adopted gravity model (i.e., $Modularity > 0$).



733

734 Figure S3. The observed interaction strength which is larger than the estimated ones from the adopted
 735 gravity model (i.e., *Modularity* < 0).
 736

737

Table S1. The results of the Rand Index (RI) analysis between each pair of the methods

	<i>City</i>	<i>Infomap</i>	<i>Louvain</i>	<i>REDCAP</i>
<i>City</i>	-	0.85	0.76	0.24
<i>Infomap</i>	-	-	0.80	0.24
<i>Louvain</i>	-	-	-	0.20
<i>REDCAP</i>	-	-	-	-

738

739

References

740 Alstott, J., Panzarasa, P., Rubinov, M., Bullmore, E.T. and Vértés, P.E. (2014). A unifying
 741 framework for measuring weighted rich clubs. *Scientific reports*, 4, 7258. doi:
 742 10.1038/srep07258

743 Batty, M. (2013). *The new science of cities*. MIT Press.

744 Blondel, V.D., Guillaume, J.L., Lambiotte, R. and Lefebvre, E. (2008). Fast unfolding of
 745 communities in large networks. *Journal of statistical mechanics: theory and*
 746 *experiment*, 2008(10), 10008. doi: 10.1088/1742-5468/2008/10/P10008

747 Burgess E.W. (2008) *The Growth of the City: An Introduction to a Research Project*. In:
 748 Marzluff J.M. et al. (eds) *Urban Ecology*. Springer, Boston, MA.
 749 https://doi.org/10.1007/978-0-387-73412-5_5.

750 Cao, S., Hu, D., Hu, Z., Zhao, W., Chen, S. and Yu, C. (2018). Comparison of spatial
 751 structures of urban agglomerations between the Beijing-Tianjin-Hebei and
 752 Boswash based on the subpixel-level impervious surface coverage product. *Journal*
 753 *of Geographical Sciences*, 28(3), 306-322. doi: 10.1007/s11442-018-1474-0

754 Castells, M. (2011). *The rise of the network society* (Vol. 12). John Wiley & sons.

755 Colizza, V., Flammini, A., Serrano, M.A. and Vespignani, A. (2006). Detecting rich-club
 756 ordering in complex networks. *Nature physics*, 2(2), 110-115. doi:
 757 10.1038/nphys209

758 Colizza, V., Pastor-Satorras, R. and Vespignani, A. (2007). Reaction–diffusion processes
759 and metapopulation models in heterogeneous networks. *Nature Physics*, 3(4), 276-
760 282. doi: 10.1038/nphys560

761 De Montis, A., Caschili, S. and Chessa, A. (2013). Commuter networks and community
762 detection: a method for planning sub regional areas. *The European Physical Journal*
763 *Special Topics*, 215(1), 75-91. doi: 10.1140/epjst/e2013-01716-4

764 Ducruet, C., Cuyala, S. and Hosni, A.E. (2016). The changing influence of city-systems on
765 global shipping networks: an empirical analysis. *Journal of Shipping and Trade*,
766 1(1), 4. doi: 10.1186/s41072-016-0006-2

767 Dugué, N. and Perez, A., 2015. Directed Louvain: maximizing modularity in directed
768 networks. Université d'Orléans.

769 Fortunato, S. (2010). Community detection in graphs. *Physics reports*, 486(3-5), 75-174.
770 doi: 10.1016/j.physrep.2009.11.002

771 Foster, J.G., Foster, D.V., Grassberger, P. and Paczuski, M. (2010). Edge direction and the
772 structure of networks. *Proceedings of the National Academy of Sciences*, 107(24),
773 10815-10820. doi: 10.1073/pnas.0912671107

774 Fotheringham, A. S. (1981). Spatial structure and distance-decay parameters. *Annals of the*
775 *Association of American Geographers*, 71(3), 425-436. doi: 10.1111/j.1467-
776 8306.1981.tb01367.x

777 Gao, S., Liu, Y., Wang, Y. and Ma, X. (2013). Discovering Spatial Interaction
778 Communities from Mobile Phone Data. *Transactions in GIS*, 17(3), 463-481. doi:
779 10.1111/tgis.12042

780 Guo, D. (2008). Regionalization with dynamically constrained agglomerative clustering
781 and partitioning (REDCAP). *International Journal of Geographical Information*
782 *Science*, 22(7), 801-823. doi: 10.1080/13658810701674970

783 Guo, D. (2009). Flow mapping and multivariate visualization of large spatial interaction
784 data. *IEEE Transactions on Visualization and Computer Graphics*, 15(6), 1041-
785 1048. doi: 10.1109/TVCG.2009.143

786 Guo, D., Jin, H., Gao, P. and Zhu, X. (2018). Detecting spatial community structure in
787 movements. *International Journal of Geographical Information Science*, 32(7),
788 1326-1347. doi: 10.1080/13658816.2018.1434889

789 Harris, C.D. and Ullman, E.L. (1945). The nature of cities. *The Annals of the American*
790 *Academy of Political and Social Science*, 242(1), 7-17.

791 Hoyt, H. (1939). The structure and growth of residential neighborhoods in American cities.
792 US Government Printing Office.

793 Huang, J., Liu, X., Zhao, P., Zhang, J. and Kwan, M.P. (2019). Interactions between bus,
794 metro, and taxi use before and after the Chinese Spring Festival. *ISPRS*
795 *International Journal of Geo-Information*, 8(10), 445. doi: 10.3390/ijgi8100445

796 Huang, Q. and Wong, D.W. (2016). Activity patterns, socioeconomic status and urban
797 spatial structure: what can social media data tell us?. *International Journal of*
798 *Geographical Information Science*, 30(9), 1873-1898. doi:
799 10.1080/13658816.2016.1145225

800 Kang, C., Zhang, Y., Ma, X. and Liu, Y. (2013). Inferring properties and revealing
801 geographical impacts of intercity mobile communication network of China using a
802 subnet data set. *International Journal of Geographical Information Science*, 27(3),
803 431-448. doi: 10.1080/13658816.2012.689838

804 Kempinska, K., Longley, P. and Shawe-Taylor, J. (2018). Interactional regions in cities:
805 making sense of flows across networked systems. *International Journal of*
806 *Geographical Information Science*, 32(7), 1348-1367. doi:
807 10.1080/13658816.2017.1418878

808 Kuang, W., Chi, W., Lu, D. and Dou, Y. (2014). A comparative analysis of megacity
809 expansions in China and the US: Patterns, rates and driving forces. *Landscape and*
810 *urban planning*, 132, 121-135. doi: 10.1016/j.landurbplan.2014.08.015

811 Leicht, E.A. and Newman, M.E. (2008). Community structure in directed networks.
812 *Physical review letters*, 100(11), 118703. doi: 10.1103/PhysRevLett.100.118703

813 Lengyel, B., Varga, A., SÁgvári, B., Jakobi, Á. and Kertész, J. (2015). Geographies of an
814 online social network. *PIOS ONE*, 10(9), e0137248. doi:
815 10.1371/journal.pone.0137248

816 Li, Y. and Phelps, N.A. (2017). Knowledge polycentricity and the evolving Yangtze River
817 Delta megalopolis. *Regional Studies*, 51(7), 1035-1047. doi:
818 10.1080/00343404.2016.1240868

819 Li, Y. and Phelps, N.A. (2019). Megalopolitan glocalization: the evolving relational
820 economic geography of intercity knowledge linkages within and beyond China's
821 Yangtze River Delta region, 2004-2014. *Urban Geography*, 40(9), 1310-1334. doi:
822 10.1080/02723638.2019.1585140

823 Liu, X., Derudder, B. and Wu, K. (2016). Measuring polycentric urban development in
824 China: An intercity transportation network perspective. *Regional Studies*, 50(8),
825 1302-1315. doi: 10.1080/00343404.2015.1004535

826 Liu, X., Gong, L., Gong, Y. and Liu, Y. (2015). Revealing travel patterns and city structure
827 with taxi trip data. *Journal of Transport Geography*, 43, 78-90. doi:
828 10.1016/j.jtrangeo.2015.01.016

829 Liu, Y., Kang, C., Gao, S., Xiao, Y. and Tian, Y. (2012). Understanding intra-urban trip
830 patterns from taxi trajectory data. *Journal of geographical systems*, 14(4), 463-483.
831 doi: 10.1007/s10109-012-0166-z

832 Liu, Y., Sui, Z., Kang, C. and Gao, Y. (2014). Uncovering patterns of inter-urban trip and
833 spatial interaction from social media check-in data. *PloS one*, 9(1), e86026. doi:
834 10.1371/journal.pone.0086026

835 Louail, T., Lenormand, M., Picornell, M., Cantú, O.G., Herranz, R., Frias-Martinez, E.,
836 Ramasco, J.J. and Barthelemy, M. (2015). Uncovering the spatial structure of
837 mobility networks. *Nature communications*, 6, 6007. doi: 10.1038/ncomms7007

838 Ma, L.J. (2005). Urban administrative restructuring, changing scale relations and local
839 economic development in China. *Political Geography*, 24(4), 477-497. doi:
840 10.1016/j.polgeo.2004.10.005

841 Newman, M.E. (2002). Assortative mixing in networks. *Physical review letters*, 89(20),
842 208701. doi: /10.1103/PhysRevLett.89.208701

843 Opsahl, T. (2009). Structure and evolution of weighted networks, Doctoral dissertation,
844 Queen Mary, University of London.

845 Opsahl, T., Colizza, V., Panzarasa, P. and Ramasco, J.J. (2008). Prominence and control:
846 the weighted rich-club effect. *Physical review letters*, 101(16), 168702. doi:
847 10.1103/PhysRevLett.101.168702

848 Rand, W. M. (1971). Objective criteria for the evaluation of clustering methods. *Journal of*
849 *the American Statistical association*, 66(336), 846-850.

850 Ratti, C., Sobolevsky, S., Calabrese, F., Andris, C., Reades, J., Martino, M., Claxton, R.
851 and Strogatz, S.H. (2010). Redrawing the map of Great Britain from a network of
852 human interactions. *PloS one*, 5(12), e14248. doi: 10.1371/journal.pone.0014248
853 Rodrigue, J.P. (2016). *The geography of transport systems*. Taylor & Francis.
854 Rosvall, M. and Bergstrom, C.T. (2008). Maps of random walks on complex networks
855 reveal community structure. *Proceedings of the National Academy of*
856 *Sciences*, 105(4), 1118-1123. doi: 10.1073/pnas.0706851105
857 Shaw, S.L., Tsou, M.H. and Ye, X. (2016). Human dynamics in the mobile and big data
858 era. *International Journal of Geographical Information Science*, 30(9), 1687-1693.
859 doi: 10.1080/13658816.2016.1164317
860 Steiger, E., Westerholt, R., Resch, B. and Zipf, A. (2015). Twitter as an indicator for
861 whereabouts of people? Correlating Twitter with UK census data. *Computers,*
862 *environment and urban systems*, 54, 255-265. doi:
863 10.1016/j.compenvurbsys.2015.09.007
864 Steinley, D. (2004). Properties of the Hubert-Arable Adjusted Rand Index. *Psychological*
865 *methods*, 9(3), 386. doi: 10.1037/1082-989X.9.3.386
866 Taylor, P.J. and Derudder, B. (2015). *World city network: a global urban analysis*.
867 Routledge.
868 Taylor, P.J., Catalano, G. and Walker, D.R. (2002). Measurement of the world city
869 network. *Urban Studies*, 39(13), 2367-2376. doi: 10.1080/00420980220080011
870 Van Den Heuvel, M.P. and Sporns, O. (2011). Rich-club organization of the human
871 connectome. *Journal of Neuroscience*, 31(44), 15775-15786. doi:
872 10.1523/JNEUROSCI.3539-11.2011
873 Wang, Y., Dong, L., Liu, Y., Huang, Z. and Liu, Y. (2019). Migration patterns in China
874 extracted from mobile positioning data. *Habitat International*, 86, 71-80. doi:
875 10.1016/j.habitatint.2019.03.002
876 Wang, Z., Zhang, F. and Wu, F. (2017). Neighbourhood cohesion under the influx of
877 migrants in Shanghai. *Environment and Planning A: Economy and Space*, 49(2),
878 407-425. doi: 10.1177/0308518X16673839
879 Wei, Y., Song, W., Xiu, C. and Zhao, Z. (2018). The rich-club phenomenon of China's
880 population flow network during the country's spring festival. *Applied*
881 *Geography*, 96, 77-85. doi: 10.1016/j.apgeog.2018.05.009
882 Wu, F. (2002). China's changing urban governance in the transition towards a more market-
883 oriented economy. *Urban Studies*, 39(7), 1071-1093. doi:
884 10.1080/00420980220135491
885 Wu, F. (2016). China's emergent city-region governance: a new form of state spatial
886 selectivity through state-orchestrated rescaling. *International Journal of Urban and*
887 *Regional Research*, 40(6), 1134-1151. doi: 10.1111/1468-2427.12437
888 Wu, F. (2020). Emerging cities and urban theories: a Chinese perspective. In *Theories and*
889 *models of urbanization* (pp. 171-182). Springer, Cham. doi: 10.1007/978-3-030-
890 36656-8_10
891 Wu, W., Wang, J. and Dai, T. (2016). The geography of cultural ties and human mobility:
892 Big data in urban contexts. *Annals of the American Association of*
893 *Geographers*, 106(3), 612-630. doi: 10.1080/00045608.2015.1121804

894 Xing, Y., Lu, J. and Chen, S. (2016). Weighted complex network analysis of shanghai rail
895 transit system. *Discrete Dynamics in Nature and Society*. 2016, 8. doi:
896 10.1155/2016/1290138

897 Xu, X.K., Zhang, J. and Small, M. (2010). Rich-club connectivity dominates assortativity
898 and transitivity of complex networks. *Physical Review E*, 82(4), 046117. doi:
899 10.1103/PhysRevE.82.046117

900 Xu, Y., Jiang, S., Li, R., Zhang, J., Zhao, J., Abbar, S. and González, M.C. (2019).
901 Unraveling environmental justice in ambient PM_{2.5} exposure in Beijing: A big
902 data approach. *Computers, Environment and Urban Systems*, 75, 12-21. doi:
903 10.1016/j.compenvurbsys.2018.12.006

904 Xu, Y., Li, J., Belyi, A. and Park, S. (2020). Characterizing destination networks through
905 mobility traces of international tourists—A case study using a nationwide mobile
906 positioning dataset. *Tourism Management*, 82, 104195. doi:
907 10.1016/j.tourman.2020.104195

908 Yeh, A.G.O. and Chen, Z. (2020). From cities to super mega city regions in China in a new
909 wave of urbanisation and economic transition: Issues and challenges. *Urban Studies*,
910 57(3), 636-654. doi: 10.1177/0042098019879566

911 Yin, J., Soliman, A., Yin, D. and Wang, S. (2017). Depicting urban boundaries from a
912 mobility network of spatial interactions: a case study of Great Britain with geo-
913 located Twitter data. *International Journal of Geographical Information
914 Science*, 31(7), 1293-1313. doi: 10.1080/13658816.2017.1282615

915 Zhang, B. (2016). Coordinated Development for the Beijing-Tianjin-Hebei Region: A
916 Strategic Trade-off in State Spatial Governance. In *Urban Planning Forum* (No. 4,
917 p. 5).

918 Zhang, W., Derudder, B., Wang, J. and Shen, W. (2018). Regionalization in the Yangtze
919 River Delta, China, from the perspective of inter-city daily mobility. *Regional
920 Studies*, 52(4), 528-54. doi: 10.1080/00343404.2017.1334878

921 Zhao, P. and Hu, H. (2019). Geographical patterns of traffic congestion in growing
922 megacities: Big data analytics from Beijing. *Cities*, 92, 164-174. doi:
923 10.1016/j.cities.2019.03.022

924 Zhao, P., Liu, X., Shi, W., Jia, T., Li, W. and Chen, M. (2018). An empirical study on the
925 intra-urban goods movement patterns using logistics big data. *International Journal
926 of Geographical Information Science*, 34(6), 1089-1116. doi:
927 10.1080/13658816.2018.1520236

928 Zhong, C., Arisona, S.M., Huang, X., Batty, M. and Schmitt, G. (2014). Detecting the
929 dynamics of urban structure through spatial network analysis. *International Journal
930 of Geographical Information Science*, 28(11), 2178-2199. doi:
931 10.1080/13658816.2014.914521

932 Zhong, C., Zeng, S., Tu, W. and Yoshida, M. (2018). Profiling the spatial structure of
933 London: from individual tweets to aggregated functional zones. *ISPRS
934 International Journal of Geo-Information*, 7(10), 386. doi: 10.3390/ijgi7100386

935 Zhu, X., Wang, Q., Zhang, P., Yu, Y. and Xie, L. (2020). Optimizing the spatial structure
936 of urban agglomeration: based on social network analysis. *Quality & Quantity*. doi:
937 10.1007/s11135-020-01016-3